FEBS Letters 567 (2004) 316–320 FEBS 28461

Insights into the specificity of RNA cleavage by the *Escherichia coli* MazF toxin

Ana J. Muñoz-Gómez[a], Sandra Santos-Sierra[a,1], Alfredo Berzal-Herranz[b], Marc Lemonnier[a,*], Ramón Díaz-Orejas[a]

[a] *Department of Molecular Microbiology, Centro de Investigaciones Biológicas CSIC, Ramiro de Maeztu 9, E-28040 Madrid, Spain*
[b] *Instituto de Parasitología y Biomedicina, López-Neyra CSIC, Ventanilla 11, E-18001 Granada, Spain*

Received 1 April 2004; revised 29 April 2004; accepted 3 May 2004

Available online 18 May 2004

Edited by Stuart Ferguson

Abstract The *mazEF* (*chpA*) toxin–antitoxin system of *Escherichia coli* is involved in the cell response to nutritional and antibiotic stresses as well as in bacterial-programmed cell death. Valuable information on the MazF toxin was derived from the determination of the crystal structure of the MazE/MazF complex and from in vivo data, suggesting that MazF promoted ribosome-dependent cleavage of messenger RNA. However, it was concluded from recent in vitro analyses using a MazF-(His6) fusion protein that MazF was an endoribonuclease that cleaved messenger RNA specifically at 5′-ACA-3′ sites situated in single-stranded regions. In contrast, our work reported here shows that native MazF protein cleaves RNA at the 5′ side of residue A in 5′-NAC-3′ sequences (where N is preferentially U or A). MazF-dependent cleavage occurred at target sequences situated either in single- or double-stranded RNA regions. These activities were neutralized by a His6-MazE antitoxin. Although essentially consistent with previous in vivo reports on the substrate specificity of MazF, our results strongly suggest that the endoribonuclease activity of MazF may be modulated by additional factors to cleave messenger and other cellular RNAs.

Keywords: Toxin–antitoxin systems; MazF (ChpAK) endoribonuclease; MazE (ChpAI) antitoxin; RNA cleavage; Bacterial programmed cell death; *Escherichia coli*

1. Introduction

Toxin–antitoxin (TA) systems are found in bacterial chromosomes and plasmids as well as in archaeal genomes [1–3]. They usually consist of two genes, arranged as an operon, that encode a toxin and its cognate antitoxin, respectively [2,4]. Plasmid-borne TA systems contribute to plasmid maintenance by preventing the growth of plasmid-free progeny, through a mechanism called post-segregational killing [5,6]. Less clear is the biological role of chromosomal TA systems. A major source of information came from the studies on the *mazEF* system (also called *chpA*) of *Escherichia coli* [7]. This system is homologous to the identical *parD* and *pem* systems found, respectively, in plasmids R1 and R100 [8,9]. *mazEF* is composed of two adjacent genes, *mazE* and *mazF*, that are located downstream of the *relA* gene [10]. MazF is a stable toxin, while MazE is a labile antitoxin degraded by the ClpPA serine protease. MazF binds to MazE and this interaction protects the cells against the toxicity of MazF [11]. The recently solved crystal structure of the MazE/MazF complex revealed that both proteins form a linear heterohexamer composed of alternating toxin and antidote homodimers ($MazF_2$–$MazE_2$–$MazF_2$). Within this complex, the interactions between MazE and MazF are primarily mediated by the C-terminal portion of MazE [12]. In addition, the combined action of MazE and MazF is required to efficiently autoregulate the *mazEF* operon at the transcriptional level [11,13]. Furthermore, the *mazEF* system was shown to mediate cell death following thymine starvation or exposure to antibiotics or toxins that inhibit transcription and/or translation [14–16]. On the other hand, overproduction of MazF in *E. coli* was shown to inhibit protein synthesis and DNA replication in vivo leading to the arrest of cell growth, all these effects being reversed by the later expression of the MazE antitoxin gene [17]. Moreover, the mechanism of action of the MazF toxin has been approached by two recent reports. The first one indicated that the in vivo overproduction of the MazF toxin induced the cleavage of translated mRNAs [18], thus closely resembling the mechanism of RelE, the toxin of the TA system *relBE* of *E. coli* that catalyzes the cleavage of specific mRNA codons at the A site of the ribosome [19,20]. The second piece of work, which was carried out in vitro using a purified histidine-tagged MazF protein (MazF-His6), indicated that this toxin was an endoribonuclease that cleaved only single-stranded RNA regions specifically at ACA sequences [21]. In essence, these reports were consistent in that MazF mediates messenger RNA cleavage to cause a block of protein synthesis in vivo. However, the finding of a ribosome-independent ribonuclease activity [21] argued against the claim that MazF cleavage exclusively involved mRNA molecules that were being translated [18]. Moreover, the RNA cleavage specificities reported in vivo for MazF [18] and in vitro for His6-MazF [21] were basically inconsistent. Here, we aimed to clarify the situation by carrying out an independent in vitro analysis of MazF

* Corresponding author. Fax: +34-91-536-0432.
E-mail address: mlm@cib.csic.es (M. Lemonnier).

[1] Present address: Institut für Biochemische Pharmakologie, Universität Innsbruck, Peter Mayr Strasse 1, A-6020 Innsbruck, Austria.

Abbreviations: TA, toxin–antitoxin; CD, circular dichroism spectroscopy

0014-5793/$22.00
doi:10.1016/j.febslet.2004.05.005

endoribonuclease activity. Our approach differs from previous studies in that we use: (i) a preparation of native MazF protein whose quality is supported by biophysical and functional evidence; (ii) a set of well-characterized natural RNA substrates; and (iii) a direct technique that allows the visualization of all the cleavage products for a given substrate. Our results show that MazF cleaves single- and double-stranded RNA at the 5′ side of residue A in 5′-NAC-3′ sequences (where N is preferentially U or A). These data are discussed in the light of the available information on the biological function of MazF.

2. Materials and methods

2.1. Protein purification

The MazF toxin and the His6-tagged MazE antitoxin were purified following a protocol identical to the one that was formerly used to purify the Kid and His6-Kis proteins [22]. The proteins were diluted in 0 mM KCl, 20 mM HEPES-KOH pH 7.8, and 100 μg ml^{-1} BSA before use.

2.2. Biophysical experiments

Sedimentation equilibrium experiments were performed with MazF at 45 μM in 100 mM sodium phosphate buffer, pH 7.0, as described [23]. Circular dichroism spectroscopy (CD) and thermal denaturation studies were carried out with MazF at 15 μM in the same buffer, as described [23].

2.3. Antitoxin–toxin interaction

The His6-MazE antitoxin (50 μg in 200 mM KCl and 20 mM imidazole, pH 8.0) was incubated with nickel-activated Sepharose beads (Amersham Biosciences) for 1 h at 4 °C, using an orbital shaker. The beads were then recovered by centrifugation at 13 000 rpm for 1 min at 4 °C in a bench centrifuge (Eppendorf) and the supernatant was discarded. To wash unbound His6-MazE, the beads were resuspended in 500 μl binding buffer and incubated at 4 °C with gentle shaking for 30 min. The beads were collected by centrifugation as above and were resuspended in 200 μl of buffer containing the MazF toxin (50 μg). The suspension was further incubated at 4 °C for 1 h with orbital shaking. Then, the beads were separated from the supernatant by centrifugation and the supernatant (S sample) was kept at 4 °C. The beads were washed extensively by repeating three times the washing step described above and were collected by centrifugation (P sample). The S and P samples were brought to the same volume of buffer and identical volumes were analyzed by SDS–PAGE (15%). The proteins in the gel were visualized by Coomassie blue staining.

2.4. Inhibition of protein synthesis in rabbit reticulocyte lysates

Reaction mixtures (10 μl) contained the components from the Rabbit Reticulocyte Lysate System (Promega): 7 μl of rabbit reticulocyte lysate, 0.2 μl of amino-acid mixture minus methionine (1 mM), 0.1 μg of luciferase control RNA, and 0.3 μl of KCl (70 mM, final concentration) complemented with 0.2 μl of RNAguard Ribonuclease Inhibitor (Amersham Biosciences). The assays were started by adding 4 μCi of [^{35}S]methionine and the MazF and/or His6-MazE proteins and were incubated for 1 h at 37 °C. The reactions were analyzed using SDS–PAGE (10%).

2.5. In vitro RNA cleavage analysis

TAR, CopA, and CopT RNAs were obtained from in vitro transcription with T7 RNA polymerase using as DNA templates: the pG3TAR plasmid [24] linearized with *Hin*dIII, for TAR RNA; PCR products derived from the pGW644 vector [25] using the pairs of primers 5′-TAATACGACTCACTATAGGCATAGCTGAATTGTTGG-3′/5′ GCCAGAAAAGCAAAAACC-3′ and 5′-TAATACGACTCACTATAGGCCAGAAAAGCAAAAACC-3′/5′-GCATAGCTGAATTGTTGG-3′ for CopA and CopT RNAs, respectively. The RNAs were 5′-end-labelled with [γ-^{32}P]ATP as described [26] and were separated on a 6% polyacrylamide gel containing 7 M Urea in TBE buffer. In vitro cleavage reactions were carried out with 1000 cpm of 5′-end-labelled RNAs in 10 mM KCl, 10 μg ml^{-1} BSA, and 2 mM HEPES, pH 7.8, in the presence of 4 units of SUPERase-In (Ambion). The purified MazF and His6-MazE proteins (1 μl) were added when appropriate and the reactions were incubated for 2 min at 37 °C. The reactions were stopped by adding formamide loading buffer and chilling quickly in dry ice. The RNAs were separated on a 8% polyacrylamide gel containing 7 M Urea in TBE buffer. The alkali ladder was prepared just before loading by incubation of 4000 cpm end-labelled RNA with 1 μg tRNA in 50 mM $NaHCO_3/Na_2CO_3$, pH 9.5, at 95 °C for 90 s. Digestions with RNaseT1 were performed using 2000 cpm RNA, 1 μg tRNA, 1 unit of RNaseT1 (Ambion) in 100 mM NaCl, 10 mM Mg-acetate, and 20 mM Tris, pH 7.5, and incubating for 5 min at 37 °C.

3. Results and discussion

3.1. Biophysical and functional validation of the MazF preparation

The native MazF protein was purified (Section 2.1) and subsequently tested in a series of biophysical and functional assays. Analysis of the association state of MazF by means of sedimentation equilibrium indicated that, at a 45 μM concentration, the protein formed a complex of $M_{w,a} \sim 24\,000$ Da (Fig. 1A). This molecular mass corresponds essentially to a dimer of MazF ($M_w = 24\,196$ Da). The low dispersion of the data and their adjustment to the theoretical curve expected for an ideal dimer were consistent with previous reports [27] and demonstrated that the sample was homogeneous at the tested concentration. In addition, the average secondary structure of MazF was analyzed by means of CD. The CD spectrum of the MazF preparation (Fig. 1B) is dominated by the α-helicoidal component (minimal values at 208 and 222 nm). Deconvolution analysis using the CDNN program predicted a contribution of the α-helicoidal component close to 23% and a higher percentage of β-strand and β-turn elements which represent up to 34% of the structure. The thermal stability of the protein, tested in the range 5–90 °C, indicated a co-operative transition to the denatured state at a T_m of 48 °C (Fig. 1C). Thus, both the well-defined CD spectrum and the co-operative transition to the denatured state of the sample indicated a well-structured and homogeneous protein preparation.

Next, we evaluated the activity of the purified MazF and His6-MazE proteins in two functional assays. First, the interaction between both proteins was tested by monitoring the specific retention of MazF by nickel-activated Sepharose beads bound to the His6-MazE antitoxin (Section 2.4). The result of this analysis indicated that indeed the MazF and His6-MazE proteins were able to tightly interact, since they formed a complex that resisted high-salt washing (Fig. 2A). In a second assay, we monitored the capacity of the MazF toxin to inhibit protein synthesis in rabbit reticulocyte lysates, an activity that has been reported [21]. This assay allows the visualization of the products of translation of a purified mRNA encoding the firefly luciferase (Section 2.5). Fig. 2B shows that the MazF toxin dramatically inhibited protein synthesis in these extracts, while preincubation of the assay with both MazF and His6-MazE at a 1:1 molar ratio completely neutralized this inhibition. It should be noted that former studies performed with a MazF-His6 protein tagged at the C-terminal end showed only partial recovery of protein synthesis upon incubation with excess His6-MazE antitoxin [21]. This suggests that a histidine-tag situated at the C-terminal portion of MazF may interfere with the functional interactions between this toxin and its cognate antitoxin. Taken together, our results demonstrate

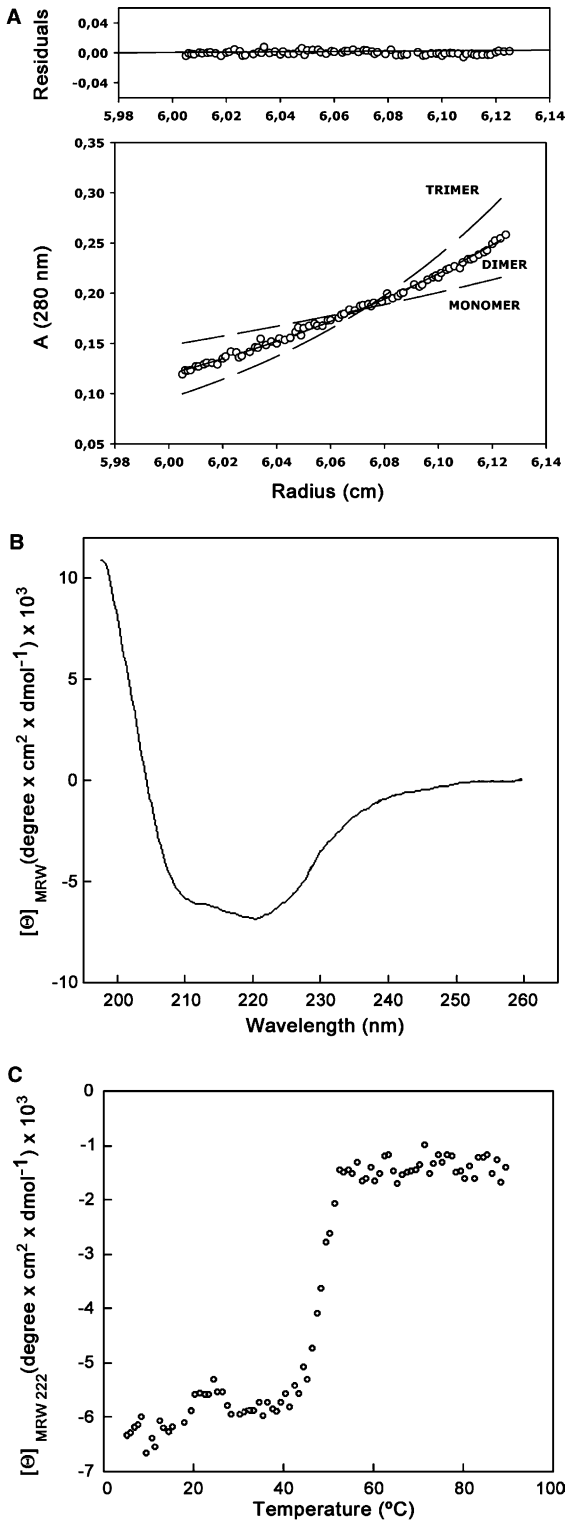

Fig. 1. Biophysical characterization of the MazF preparation. (A) Analytical centrifugation at equilibrium. Lower panel: sedimentation equilibrium gradients obtained with 45 μM MazF at 19 000 rpm, 20 °C in 100 mM sodium phosphate buffer. The solid line represents the best fit of the experimental data to a single ideal dimeric species ($M_w = 24196$ Da). Dashed lines correspond to the theoretical fit to monomer ($M_w = 12098$ Da) and trimer ($M_w = 36294$ Da). The residuals of the fit are shown in the upper panel. (B) Circular dichroism spectrum and (C) thermal denaturation profile of the MazF toxin (15 μM) in 100 mM sodium phosphate, pH 7.0.

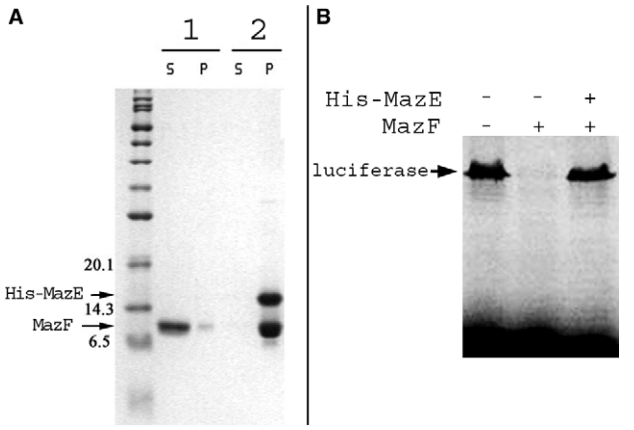

Fig. 2. Functional assays using MazF. (A) Antitoxin–toxin interaction. The His6-MazE protein (50 μg) bound to nickel-activated Sepharose beads was incubated with the MazF protein (50 μg) as described in Section 2. The beads were separated from the supernatant (S sample) by centrifugation and were finally collected after extensive washing (P sample). The S and P samples were analyzed by SDS–PAGE (15%). 1, MazF toxin incubated with nickel-activated Sepharose beads in the absence of His6-MazE; 2, MazF toxin incubated with nickel-activated Sepharose beads bound to the His6-MazE antitoxin. The leftmost lane is the Protein Molecular Weight Marker Broad Range (New England Biolabs). The bands corresponding to M_w (kDa) 6.5, 14.3, and 20.1 are indicated. (B) Protein synthesis in rabbit reticulocyte lysates using luciferase mRNA as template (see Section 2). ^{35}S-labelled protein products were analyzed using SDS–PAGE (10%). When indicated, the reactions were incubated with MazF or His6-MazE, each at 0.3 μM.

that the MazF and His6-MazE proteins used in the present study were well folded and fully active.

3.2. RNA cleavage assays

MazF and His6-MazE were tested in RNA cleavage assays using a panel of three small model RNA molecules that have been extensively characterized at the structural and functional levels, and that possess significant differences in their primary and secondary structures: the HIV-1 *trans*-activation response element TAR [28], the CopA antisense RNA and its target RNA CopT of plasmid R1 [29]. The three RNAs were 5′-end-labelled with ^{32}P, purified, and challenged with increasing amounts of the purified MazF toxin prior to being fractionated by electrophoresis. RNA samples treated either with alkali or with RNAseT1 were also included to allow the precise mapping of the cleavage sites. TAR, CopA, and CopT were cleaved by the MazF toxin at three, two, and seven different sites, respectively (Fig. 3A and B). Cleavage was not observed when MazF was provided together with the His6-MazE antitoxin, thus indicating that the activity was specific. Analysis of the RNA sequences around the cleavage sites showed that MazF always cleaved at the 5′ end of 5′-AC-3′ sequences (Fig. 3B and C). The nucleotides situated at the 5′ of the cleavage sites were, in 10 out of 12 cases, A or U. In contrast, there was no significant conservation of the residue immediately at 3′ of the target 5′-AC-3′ sequence (Fig. 3C). Interestingly, the cleavage sites were predominantly, but not always, situated in single-stranded RNA regions (Fig. 3B). For example, the two copies of 5′-AAC-3′ present in TAR (filled square and circle, Fig. 3B) were cleaved by MazF, albeit being located in single- and double-stranded regions, respectively (the same occurred with the two 5′-UAC-3′ sites in CopT). However, inasmuch as the intensities of the bands visualized in Fig. 3A reflect the

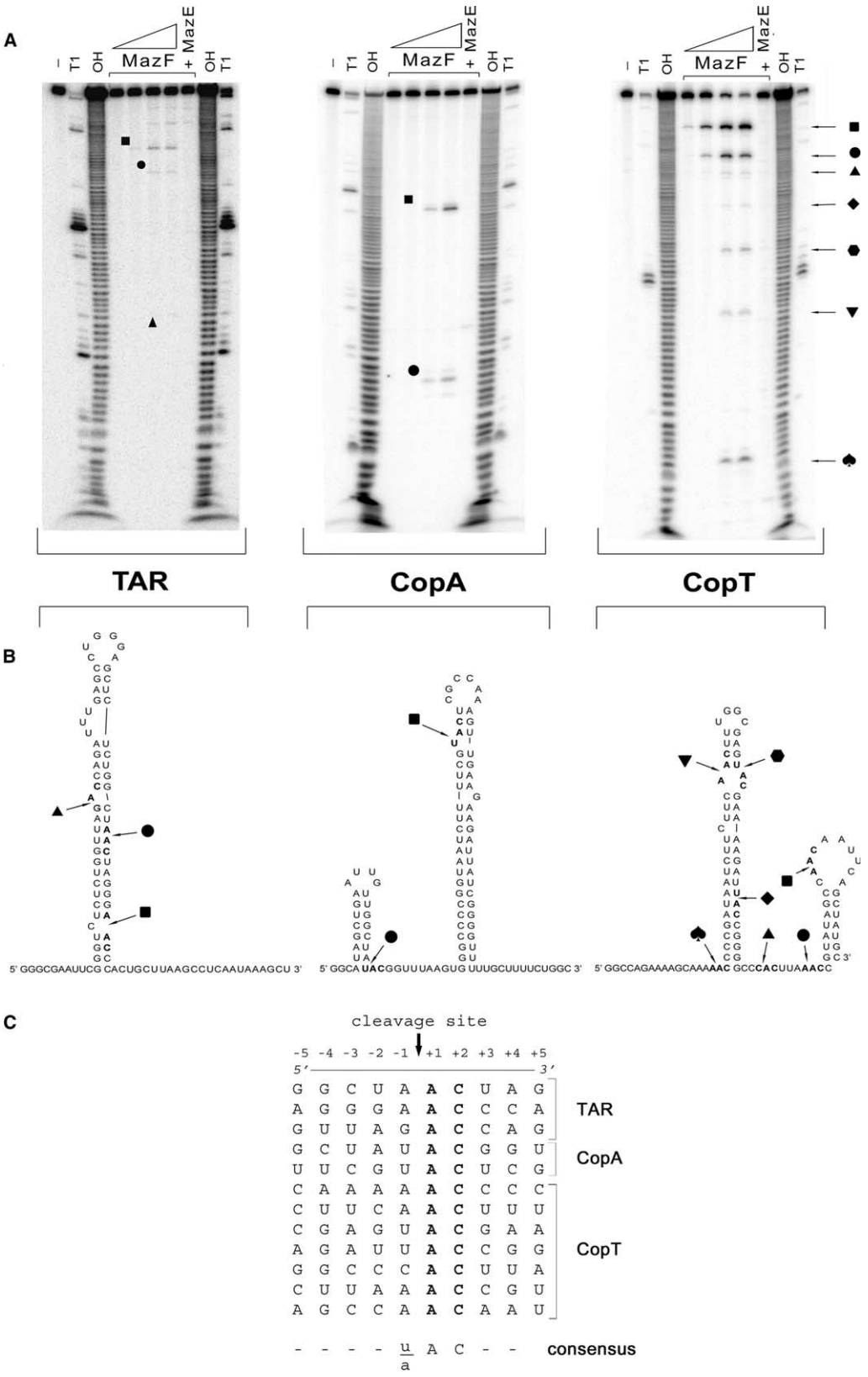

Fig. 3. In vitro RNA cleavage by MazF. (A) 5′-^{32}P-labelled RNAs TAR, CopA, and CopT were incubated with increasing amounts (0.005, 0.05, 0.5, and 1 μM, respectively) of MazF protein prior to being fractionated by electrophoresis. Where indicated, MazE was added with MazF (1 μM each). MazF cleavage sites are indicated by solid symbols. -, OH and T1 denote samples that were non-treated, partially hydrolyzed with alkali and digested with RNase T1, respectively. (B) Secondary structures of TAR, CopA, and CopT RNAs and their respective MazF cleavage sites. Symbols are as indicated in panel A. (C) A summary of the MazF cleavage sites and their neighboring RNA sequences.

accessibility of a given RNA site to the cleavage activity of MazF, the sequences located in single-stranded regions seemed to be first-choice sites for MazF. Therefore, from this study it can be concluded that MazF cleaves single- and double-stranded RNA with a marked preference for 5′-(U/A)AC-3′ sequences in single-stranded RNA. Our findings are basically consistent with the previous report of the in vitro endoribonuclease activity of MazF by Zhang et al. [21]. However, these authors claim that MazF cleaves mRNA specifically at 5′-ACA-3′ sequences only in single-stranded regions. Our present results do not support these conclusions. In contrast, three lines of evidence argue in favor of our observations: (i) all the 5′-(U/A)AC-3′ sites present in TAR, CopA or CopT RNAs were cut by MazF, with no exception (this work; Fig. 3B); (ii) 5′-AAC-3′ present in the *E. coli* tmRNA was a strong cleavage site for MazF in vivo [18]; and (iii) although presented as an exception rather than a rule, Zhang et al. [21] also show that the *lacZ* mRNA is cleaved by MazF between the U and A residues in a 5′-UAC-3′ site. However, the reasons for the discrepancy between the work reported here and that of Zhang and co-workers are unclear. As mentioned above, we use the native MazF toxin in our RNA cleavage assays, while these authors used a toxin with a histidine-tag at its C-terminal end [21]. However, while this C-terminal extension could potentially affect the binding of MazF to its natural RNA target, or to its cognate antitoxin (see Section 3.1), one would expect a disruption of the endoribonuclease activity rather that the acquisition of a new substrate specificity. Probably, the endoribonuclease activity of MazF is subject to subtle modulation by additional factors, i.e., the sequence environment and/or the secondary-structure of its RNA target. In this respect, the technique that we use to monitor RNA cleavage is specially adapted inasmuch as we visualize all the possible cleavage products for a specific RNA substrate, thus leading to a more comprehensive view of the ribonuclease activity of MazF. In particular, our results demonstrate that MazF also cleaves sequences that are situated in double-stranded RNA regions. At present we do not know whether this results from the local melting of RNA upon binding of MazF to distal sequences, that then permits subsequent cleavage, or whether MazF actually binds double-stranded RNA and specifically cleaves the target strand. Certainly, addressing this issue will benefit from the future resolution of MazF/RNA complexes at the structural level.

Moreover, in vivo experiments carried out by overexpressing the native *mazF* gene indicated that the RNA cleavage by MazF occurs not only at 5′-NAC-3′ sites [18,21], thus further supporting our view that the intrinsic activity of MazF is subject to additional controls. Possibly, the in vivo function of MazF is determined by its interaction with particular host factors (e.g., components of the translation machinery) in response to specific physiological stimuli, as previously suggested [18]. However, the relaxed substrate specificity of MazF and the fact that cleavage occurs in a ribosome-independent manner suggest that the ribonuclease activity of MazF may not be restricted to targeting messenger RNA, but rather involves the regulation of a larger panel of RNA-dependent cellular processes. Our group is currently approaching this issue.

Acknowledgements: We thank R. Giraldo for helpful support, discussions, and critical reading of the manuscript; V. Augustin and C. Pardo-Abarrio for excellent technical assistance; M. Suzanne for critical reading of the manuscript; and A. Barroso, E. Puerta, and C. Romero for helpful discussions. This work was supported by grants from the European Union (QLK2-CT-2000-00634), the Spanish Ministerio de Educación y Cultura (BIO99-0859-CO3), the Ministerio de Ciencia y Tecnología (SAF-2002-04649), the "Programa de Grupos Estratégicos de la Comunidad de Madrid", and the Spanish REIPI Network of the "Fondo de Investigaciones Sanitarias".

References

[1] Mittenhuber, G. (1999) J. Mol. Microbiol. Biotechnol. 1, 295–302.
[2] Gerdes, K. (2000) J. Bacteriol. 182, 561–572.
[3] Anantharaman, V. and Aravind, L. (2003) Genome Biol. 4, R81.
[4] Engelberg-Kulka, H. and Glaser, G. (1999) Annu. Rev. Microbiol. 53, 43–70.
[5] Holcik, M. and Iyer, V.N. (1997) Microbiology 143, 3403–3416.
[6] Gerdes, K., Rasmussen, P.B. and Molin, S. (1986) Proc. Natl. Acad. Sci. USA 83, 3116–3120.
[7] Masuda, Y., Miyakawa, K., Nishimura, Y. and Ohtsubo, E. (1993) J. Bacteriol. 175, 6850–6856.
[8] Bravo, A., de Torrontegui, G. and Diaz, R. (1987) Mol. Gen. Genet. 210, 101–110.
[9] Tsuchimoto, S., Ohtsubo, H. and Ohtsubo, E. (1988) J. Bacteriol. 170, 1461–1466.
[10] Metzger, S., Dror, I.B., Aizenman, E., Schreiber, G., Toone, M., Friesen, J.D., Cashel, M. and Glaser, G. (1988) J. Biol. Chem. 263, 15699–15704.
[11] Aizenman, E., Engelberg-Kulka, H. and Glaser, G. (1996) Proc. Natl. Acad. Sci. USA 93, 6059–6063.
[12] Kamada, K., Hanaoka, F. and Burley, S.K. (2003) Mol. Cell 11, 875–884.
[13] Marianovsky, I., Aizenman, E., Engelberg-Kulka, H. and Glaser, G. (2001) J. Biol. Chem. 276, 5975–5984.
[14] Hazan, R., Sat, B., Reches, M. and Engelberg-Kulka, H. (2001) J. Bacteriol. 183, 2046–2050.
[15] Sat, B., Hazan, R., Fisher, T., Khaner, H., Glaser, G. and Engelberg-Kulka, H. (2001) J. Bacteriol. 183, 2041–2045.
[16] Sat, B., Reches, M. and Engelberg-Kulka, H. (2003) J. Bacteriol. 185, 1803–1807.
[17] Pedersen, K., Christensen, S.K. and Gerdes, K. (2002) Mol. Microbiol. 45, 501–510.
[18] Christensen, S.K., Pedersen, K., Hansen, F.G. and Gerdes, K. (2003) J. Mol. Biol. 332, 809–819.
[19] Christensen, S.K. and Gerdes, K. (2003) Mol. Microbiol. 48, 1389–1400.
[20] Pedersen, K., Zavialov, A.V., Pavlov, M.Y., Elf, J., Gerdes, K. and Ehrenberg, M. (2003) Cell 112, 131–140.
[21] Zhang, Y., Zhang, J., Hoeflich, K.P., Ikura, M., Qing, G. and Inouye, M. (2003) Mol. Cell 12, 913–923.
[22] Hargreaves, D., Giraldo, R., Santos-Sierra, S., Boelens, R., Rice, D.W., Díaz-Orejas, R. and Rafferty, J.B. (2002) Acta Crystallogr., Sect. D 58, 355–358.
[23] Santos-Sierra, S., Lemonnier, M., Nunez, B., Hargreaves, D., Rafferty, J., Giraldo, R., Andreu, J.M. and Diaz-Orejas, R. (2003) Plasmid 50, 120–130.
[24] Perez-Ruiz, M., Sievers, D., Garcia-Lopez, P.A. and Berzal-Herranz, A. (1999) Antisense Nucleic Acid Drug Dev. 9, 33–42.
[25] Persson, C., Wagner, E.G. and Nordstrom, K. (1988) EMBO J. 7, 3279–3288.
[26] Barroso-delJesus, A., Tabler, M. and Berzal-Herranz, A. (1999) Antisense Nucleic Acid Drug Dev. 9, 433–440.
[27] Zhang, J., Zhang, Y. and Inouye, M. (2003) J. Biol. Chem. 278, 32300–32306.
[28] Karn, J. (1999) J. Mol. Biol. 293, 235–254.
[29] Wagner, G.E.H. and Brantl, S. (1998) Trends Biochem. Sci. 23, 451–454.